

P. Kosoboutskyy, M. Karkulovska
Department of Computer-Aided Design (CAD)
Department of Physics (DP)
Lviv Polytechnic National University

SUPPRESSION OF INTERFACE IMPEDANCE CONTRAST IN PLANE-PARALLEL COATINGS

© *Kosoboutskyy P., Karkulovska M., 2015*

Досліджено спектральні та кутові умови для просвітлення границь за допомогою подавлення імпедансного контрасту, застосовуючи метод теоретичного і комп'ютерного аналізу функції обвідних спектрів багатопроменевої інтерференції. Дослідження проводились у резонансній області дисперсії діелектричної проникності в одинарних та бінарних плоско паралельних структурах. Одержані аналітичні співвідношення між кутом Брюстера/псевдо-Брюстера і параметрами структури.

Ключові слова: спектри нормального та похилого відбивання, багатопроменева інтерференція, кут Брюстера кут псевдо-Брюстера, тонкі плівки, просвітлюючий діелектричний шар.

The paper focuses on the study of spectral and angular conditions for interface antireflection by means of impedance contrast suppression, applying the method of theoretical and computer analysis of the envelope functions of spectra of multibeam interference. The research is conducted in the resonance dispersion region of dielectric constant of the single and binary boundaries that form a plane-parallel structure. The analytical relations between the Brewster/Pseudo-Brewster angles and structure parameters are.

Key words: spectra of normal and oblique reflection, multi-beam interference, Brewster and pseudo Brewster angle, thin films, antireflection of dielectric layer.

Introduction

Interference structures are widely used for creation of effective coatings in solar energy [1–3]; highly sensitive optic-fiber microcantilever systems [4]; sensors of physical fields [5, 6, 8]; biosensors [7], etc. There are a number of applications where it is topical to take into account energy absorption of electromagnetic wave in interference structure [9], in particular it concerns the ones with multilayer coatings specially designed for electromagnetic compatibility of radio-electronic equipment and protection of the human body from the negative impact [10–12].

Properties of multilayer structures strongly depend on the geometry of electromagnetic wave falling on the object, since in this case Fresnel interface reflection coefficients and effective optical thickness of the layers change. Therefore resonant structures exhibit the properties of the spatial selection of incident waves and the modulation of spectral and angular position of the interference extrema in the reflection and transmission spectra allows creating a class of radio-optical devices [13]. Due to the implementation of total internal reflection effect at large angles of incidence, high Q-values (quality factor) of resonance peaks are obtained for a small number of layers.

Two types of the impedance contrast suppression (ICS) can be singled out for single boundaries on both sides of the interferometer as a plane-parallel plate. The first is achieved by alignment of dielectric permittivity of intersect media and is typically implemented in the frequency spectra [14], and the second is achieved as a result of the Brewster character arising out at oblique wave reflection at the interface of media with different impedances [15].

However, the antireflection of single boundary is not always accompanied by the antireflection of binary boundary as a system of two spaced parallel plate surfaces. Thus, given the multipath Fabry-Perot interference envelope minima vanishes $R_m \rightarrow 0$ in transparent structures or goes to a minimum

$R_m \rightarrow \min$ in absorbing structures and the wave phase shift is $\frac{\phi_{01} \pm (\phi_{12} - \text{Re } \tilde{\delta})}{2} = (2\ell \pm 1) \frac{\pi}{2}$,

$\ell = 0, 1, 2, 3, \dots$, the system of two Brewster angles does not reflect waves [16] and becomes invisible to this waveband and vice versa, it is maximum transparent to the incident radiation, which is important for the creation of high performance coatings, including solar energy converters. In the research work [17] the analogy between the antireflection of single (Brewster) and binary boundaries is justified. Binary boundaries can develop for *s*- and *p*- polarizations, therefore is classified as pseudo Brewster. Based on the suppression of thin films, Abeles [18] developed non-destructive method for determining the dielectric parameters of surface coatings for oblique incidence of waves on a transparent structure [19,20].

The aim of this work is to determine general manifestations in the amplitude and phase reflection spectra of suppression effects by single and binary boundaries and to establish the relations between the respective frequencies and the ICS angles and parameters of intersect media which is quite important for the technology of multi-film covering design.

II. Model and main relations

Given that two **semiinfinited** isotropic media with plane surfaces form a plane-parallel system of thickness d . Given that the transparent medium with a source of electromagnetic waves (index 0) has a dielectric constant layer $\varepsilon_0 = n_0^2$ and intersects a layer of the geometric thickness d and a dielectric constant $\tilde{\varepsilon}_1 = n_1^2$ (index of the medium 1), which is deposited on the surface of the substrate with a dielectric constant $\varepsilon_2 = n_2^2$ (index of the medium 2). Then the boundary medium-layer will have the index 01, and the layer-substrate – 12.

From the standpoint of the envelope maxima (M) and minima (m) of the multi-beam Fabry-Perot interference, the relative values of the energy reflection coefficient R are conveniently expressed as [21–23]:

$$\frac{R}{R_m} = \frac{1 + b^2 \cos^2 \Delta^- / R_m}{1 + b^2 \cos^2 \Delta^+} \quad \text{or} \quad \frac{R}{R_M} = \frac{1 - a^2 \sin^2 \Delta^- / R_M}{1 - a^2 \sin^2 \Delta^+}, \quad (1)$$

where $\tilde{r}_{01,12} = \sigma_{01,12} \exp(-i\phi_{01,12})$ amplitude coefficients of waves reflections by single boundaries 01 and 12, which at an arbitrary angle of incidence α are defined by the known Fresnel formulas [16],

$$\sigma_{01,12}^2 = \text{Re}^2 \tilde{r}_{01,12} + \text{Im}^2 \tilde{r}_{01,12}, \quad a^2 = \frac{4\sigma_{01}\Theta}{(1 + \sigma_{01}\Theta)^2}, \quad b^2 = \frac{4\sigma_{01}\Theta}{(1 - \sigma_{01}\Theta)^2}, \quad \Delta^\pm = \frac{\phi_{01} \pm (\phi_{12} - \text{Re } \tilde{\delta})}{2},$$

$\Omega = \exp(-\text{Im } \tilde{\delta})$, $\Theta = \sigma_{12}\Omega$, $\tilde{\delta} = \frac{4\pi \tilde{n}_1 d}{\lambda} \cos \tilde{\beta}_1$ – phase shift of the wave in the layer, incident on it at the

angle α and refracted in accordance with the law $n_0 \sin \alpha = \tilde{n}_1 \sin \tilde{\beta}_1$. Then for the arbitrary geometry of experiment, the level of absorption and polarization of the waves, the extrema envelope functions $R_{m,M}$ have the analytical form

$$R_{M,m} = \left(\frac{\sigma_{01} \pm \Theta}{1 \pm \sigma_{01}\Theta} \right)^2 \quad (2)$$

The widely used assessment of the quality of the interference pattern is calculated as the ratio $\frac{R_M - R_m}{R_M + R_m}$. However, as follows from (2), it is more convenient to define it as the ratio $\frac{\sqrt{R_M} - \sqrt{R_m}}{\sqrt{R_M} + \sqrt{R_m}}$.

Then $\frac{\sqrt{R_M} - \sqrt{R_m}}{\sqrt{R_M} + \sqrt{R_m}} = 2 \frac{\Theta(1 - \sigma_{01}^2)}{1 - \Theta\sigma_{01}^2}$ and with decreasing of absorption $\text{Im}\delta \rightarrow 0$, $\Omega \rightarrow 1$ contrast

$\frac{\sqrt{R_M} - \sqrt{R_m}}{\sqrt{R_M} + \sqrt{R_m}} \rightarrow 2$, whereas given that $\Omega \rightarrow 0$, $\frac{\sqrt{R_M} - \sqrt{R_m}}{\sqrt{R_M} + \sqrt{R_m}} \rightarrow 0$. The intermediate contrast

$\frac{\sqrt{R_M} - \sqrt{R_m}}{\sqrt{R_M} + \sqrt{R_m}} = 1$ is realized in the absorbing interferometers provided that $\Theta = \frac{1}{2 - \sigma_{01}^2}$. It does not make

sense to implement the similar for a phase spectra, as they are indefinite accurate within an integral number 2π . For the phase spectra of extrema envelopes $\phi_{m,M}$ they are described by functions

$$\phi_{M,m} \cong 2\pi \pm \frac{\sigma_{01}(1 - \sigma_{12}\Theta)\sin\phi_{01} + \sigma_{12}(1 - \sigma_{01}^2)\Omega}{\sigma_{01}(1 + \Theta^2)\cos\phi_{01}}, \quad (3)$$

given $\phi_{01,12} \cong m\pi$, it can be simplified as $\phi_{M,m} \approx 2\pi \pm \frac{(1 - \sigma_{01}^2)\Theta}{\sigma_{01}(1 + \Theta^2)}$.

III. Findings and discussion.

Let us introduce the difference function

$$\Delta R = R_M - R_m = 2\sigma_{01}\Theta \frac{(1 - \sigma_{01}^2)(1 - \Theta^2)}{(1 - \sigma_{01}^2\Theta^2)^2}, \quad (a)$$

$$\Delta T = T_M - T_m = \frac{4n_2 \cos\beta_2}{n_0 \cos\alpha} \frac{\sigma_{01}}{\sigma_{12}} T_{01}T_{12} \left(\frac{\Theta}{1 - \sigma_{01}^2\Theta^2} \right)^2, \quad (b)$$

$$\Delta\phi = \phi_M - \phi_m = 2 \frac{(1 - \sigma_{01}^2)\Theta}{\sigma_{01}(1 + \Theta^2)}. \quad (c)$$

In the mathematical model (4) with the rise of the level of absorption of the wave by plane-parallel layer, the width of intervals (4) decreases and given $\Omega \rightarrow 0$ and the circuits of the envelopes intersect $\Delta(R, T, \phi) \rightarrow 0$. In transparent structures the touch point of envelopes $R_m = R_M$, $T_m = T_M$, $\phi_m = \phi_M$ are formed in the ICS areas for one of layer surfaces separately

$$\sigma_{01,12} \rightarrow 0 \quad (5)$$

or for both together. The common property of the ICS is the fact that they suppress the multi-beam Fabry-Perot interference and the circuits of wave reflection by the layer $R_{\sigma_{01,12} \rightarrow 0}$, clean substrate surface

$R_{sub, \sigma_{01,12} \rightarrow 0}$ and envelopes $R_{m,M, \sigma_{01,12} \rightarrow 0}$ intersect at one point:

$$R_{\sigma_{01,12} \rightarrow 0} = R_{m,M, \sigma_{01,12} \rightarrow 0} = R_{sub, \sigma_{01,12} \rightarrow 0}. \quad (6)$$

The condition (6) does not depend on the layer thickness and the equation $R_{\sigma_{01,12} \rightarrow 0} = R_{sub, \sigma_{01,12} \rightarrow 0}$ is known as Abeles condition [18].

Theoretically, in its physical essence, the manifestation of the ICS type (5), is common for the frequency and angular spectra. For oblique reflection spectra the condition (6) is $T_{\sigma_{01,12} \rightarrow 0} = T_{m,M, \sigma_{01,12} \rightarrow 0}$.

As follows from (4c) in the ICS area of the angle $0I$ the difference function is $\Delta\phi \neq 0$.

At the points of the spectrum, in which circuits intersect

$$\sigma_{01} = \Theta, \quad (7)$$

the antireflection envelope area of R_m minima is formed. In transparent structures $\Omega = 1$ antireflection areas are caused by the intersection of the dispersion circuits of modules.

$$\sigma_{01} = \sigma_{12}. \quad (8)$$

In absorbent structures the suppression by absorption of wave reflection by inner boundary σ_{12} may lead to creation of another area of antireflection under the following condition

$$\sigma_{12}\Omega \rightarrow \sigma_{01}. \quad (9)$$

Full antireflection of layer occurs when both of the equations are solved:

$$\begin{aligned} R_m &= 0 & (a) \\ b^2 \cos^2 \Delta^+ &= 0 & (b) \end{aligned} \quad (10)$$

The condition (10a) is equivalent to (7), and (10b) – wave phase shift $\Delta^+ = (2\ell \pm 1)\frac{\pi}{2}$, $\ell = 0, 1, 2, 3, \dots$

The research findings are valid not only for electromagnetic, but also for acoustic waves, of plane and other types, to which the Fabry-Perot principle can be applied. The analysis of the numerical calculations of phase spectra for the wave let through a layer showed that they are not sensitive or low-sensitive to ICS of single and binary boundaries.

Single boundary. In resonant region the Lorentz oscillator has been chosen as the model of dielectric function dispersion:

$$\tilde{n}_1^2 = \varepsilon_0 + \frac{4\pi\tilde{\lambda}\omega_0^2}{\omega_0^2 - \omega^2 - i\omega\gamma} = (n_1 - i\chi_1)^2, \quad (11)$$

where ε_0 – background dielectric constant at low frequencies; $4\pi\tilde{\lambda}$ – transition oscillator strength in the resonant state with the frequency of ω_0 , γ – decaying parameter. In frequency range $\omega_{i01,12}$, the absorption level is relatively small, therefore the ICS is conditioned by alignment indexes for the refractions contacting with the media layer (figure 1).

Let us define frequencies $\omega_{i01,12}$. Away from the resonance frequency as a rule $n_1 \gg \chi_1$ and $\text{Re} \tilde{\varepsilon} \gg \text{Im} \tilde{\varepsilon}$. Therefore, from the system of the equations $n_{0,2}^2 \cong n_1^2(\omega_{i01,12})$ we obtain that

$$\omega_{i,01,12} \cong \omega_0 \sqrt{1 + \frac{4\pi\tilde{\lambda}}{\varepsilon_0 - n_{0,2}^2}}, \quad (12)$$

At oblique incidence of p -wave single boundaries have similar properties of the ICS at the frequencies $\omega_{i01,12}$ at Brewster angles $\alpha_{p01,12}$, that are connected with media parameters Abeles invariants [18]:

$$\begin{aligned} \left(\frac{1}{n_0^2} + \frac{1}{n_1^2} \right) \sin^2 \alpha_{p01} &= \frac{1}{n_0^2} & (a) \\ \left(\frac{1}{n_1^2} + \frac{1}{n_2^2} \right) \sin^2 \alpha_{p12} &= \frac{1}{n_0^2} & (b) \end{aligned} \quad (13)$$

The first (13a) refers to the boundary with indices 01 , and the second (13b) with index 12 . The angle α_{p01} is always valid, whereas α_{p12} can be imaginary. For the clean substrate surface, Abeles invariant is

$$\left(\frac{1}{n_0^2} + \frac{1}{n_2^2} \right) \sin^2 \alpha_{psub} = \frac{1}{n_0^2}, \text{ where } \alpha_{psub} \text{ is a corresponding Brewster angle.}$$

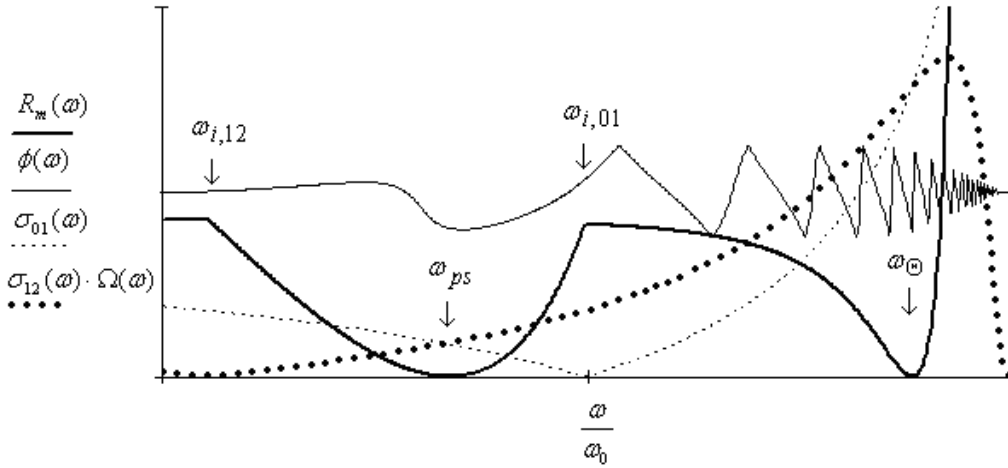


Fig. 1. Fragments of calculated frequency reflection circuits R , envelopes $R_{m,M}$ clean substrate surface R_{sub} of the wave by a single layer with parameters $n_0 = 2.9$ and $n_2 = 2.7$

The well known Abeles invariants do not reflect the connection of the media parameters with the power reflection coefficients at the tangency points of the envelopes. The system of equations that describes such connection is as follows

$$\frac{1}{n_1^2} \frac{\cos^2 \alpha_{p12}}{(1 - R_{psub}(\alpha = \alpha_{p12}))^2} = \frac{1}{n_1^4} \frac{n_1^2 - n_0^2 \sin^2 \alpha_{p12}}{(1 + R_{psub}(\alpha = \alpha_{p12}))^2}; \quad (14)$$

$$\frac{n_1^2 - n_0^2 \sin^2 \alpha_{p01}}{(1 - R_{psub}(\alpha = \alpha_{p01}))^2} = \frac{1}{n_2^4} \frac{n_2^2 - n_0^2 \sin^2 \alpha_{p01}}{(1 + R_{psub}(\alpha = \alpha_{p01}))^2}.$$

At oblique incidence, the patterns of phase spectra change in the ICS areas are analogical to the corresponding, above described in the frequency spectra at normal incidence.

Binary boundary. The antireflection of the envelope R_m is formed in the areas in which the conditions of the ICS (8) and (9) are met. At normal incidence, the equation (9) is satisfied in the transparency level or weak wave absorption layer. Then from the equality $R_m = 0$ the conditions of antireflection of envelope minima of the Fabry-Perot interference follow

$$n_0 n_2 = n_1^2, \quad n_0 \rangle n_1 \rangle n_2, n_0 \langle n_1 \langle n_2, \quad (a); \quad (15)$$

$$n_0 = n_2, \quad n_0 \rangle n_1 \langle n_2, n_0 \langle n_1 \rangle n_2, \quad (b).$$

The equation (15,a) fully reflects the ICS layer condition and is manifested in the form of antireflection of envelope circuit R_m , contacting with the media having different dielectric properties (unbalanced condition of the structure $n_0 \neq n_2$). The equality (15,b) reflects the ICS structure and antireflection of the circuit R_m in a symmetric state $n_0 = n_2$. Let us indicate the given frequencies as ω_{ps} and define them.

If we neglect the absorption in the layer, then from the equality $\Lambda \cong \varepsilon_0 + \frac{4\pi\tilde{\lambda}\omega_0^2}{\omega_0^2 - \omega_{ps}^2}$ we have

$$\omega_{ps} \cong \omega_0 \sqrt{1 + \frac{4\pi\tilde{\lambda}}{\varepsilon_0 - \Lambda}}, \quad (16)$$

where $\Lambda = n_0 n_2$ for the condition (15,a) and $\Lambda = n_{0,2}^2$ – (15,b).

It is important to emphasize that in the area of structure transition in a symmetric state $n_0 = n_2$, the frequency (16) moves to one of the frequencies (12).

Another type of ICS layer occurs at the frequency ω_{Θ} . In the area of increasing absorption the condition (9) may be carried out, although the equation (15,a) is not satisfied. The antireflection frequency ω_{Θ} of the circuit R_m is:

$$\omega_{\Theta} \cong \frac{c_0}{2\chi_{1\omega_{\Theta}} d} \ln \frac{\sigma_{01,\omega_{\Theta}}}{\sigma_{12,\omega_{\Theta}}}, \quad (17)$$

where c_0 – speed of light in vacuum, $\sigma_{01,\omega_{\Theta}}^2 = \left(\frac{n_0 - n_1(\omega_{\Theta})}{n_0 + n_1(\omega_{\Theta})} \right)^2$, $\sigma_{12,\omega_{\Theta}}^2 = \left(\frac{n_1(\omega_{\Theta}) - n_2}{n_1(\omega_{\Theta}) + n_2} \right)^2$.

In oblique geometry the conditions of envelope minima of the Fabry-Perot interference (15) are not satisfied either. In order to formulate them, we express the Fresnel coefficients in terms of the effective

refractive index $N_{p,sj} = \begin{cases} n_j / \cos \beta_j, \\ n_j \cdot \cos \beta_j, \end{cases} \quad j = 0,1,2$ [16]. Then the conditions (15) are:

$$N_0 N_2 = N_1^2, \quad N_0 \rangle N_1 \rangle N_2, \quad N_0 \langle N_1 \langle N_2, \quad (a);$$

$$N_0 = N_2, \quad N_0 \rangle N_1 \langle N_2, \quad N_0 \langle N_1 \rangle N_2, \quad (b).$$

The equation (18,a) is valid for both polarization components of light, whereas (18,b) is valid only for the p -wave. However, unlike (15), they have fundamentally different physical nature. For example, for the structure with a ratio of refractive index $n_1^2 = n_0 n_2$, the envelope R_{pm} is antireflected under condition (18,b).

Let us denote the angle of circuit antireflection R_{pm} as α_{ps} for p -wave, circuit R_{sm} as α_{ss} for s -polarization. The angles α_{ps} , as the solutions to equation (18,a) are

$$\alpha_{ps1,2} = a \sin \frac{1}{n_0} \sqrt{\left(A \pm \sqrt{A^2 - B} \right)}, \quad (19)$$

where $A = \frac{n_1^2 - \frac{1}{2} \frac{n_1^8}{n_0^2 n_2^2 \sin^2 \alpha_{psub}}}{1 - \frac{n_1^8}{n_0^4 n_2^4}}$, $B = \frac{n_1^4}{1 + \frac{n_1^4}{n_0^2 n_2^2}}$. The equation (18,b), has the solution

$$\alpha_{psub} = a \sin \left(\frac{n_0 n_2}{\sqrt{n_0^2 + n_2^2}} \right), \quad (20)$$

which coincides with the Brewster angle for a clean substrate surface. For s – wave the Brewster effect is not observed and the physical meaning of the equation has a solution (18,a)

$$\sin \alpha_{ss} = \sqrt{\frac{n_1^4 - n_0^2 n_2^2}{n_0^2 (2n_1^2 - n_0^2 - n_2^2)}}. \quad (21)$$

The angles α_{ps}, α_{ss} may be real or complex, as well as hidden by total internal reflection at the boundary 01, depending on the ratio between the refractive indexes.

Fig. 2 presents the results of a numerical calculation of circuits R_{pm}, R_{psub} and difference functions $\Delta N_{01,12} = N_{0,1} - N_{1,2}$, $\Delta N_{ps} = N_{p1}^2 - N_{p0} N_{p2}$, $\Delta N_{psub} = N_{p1}^2 - N_{p0} - N_{p2}$, confirming the adequacy of conditions for the oblique geometry (18) and not for (15). For a given set of values of the refractive index both antireflection angles (19) and $\alpha_{p01} > \alpha_{p12}$ are valid and hidden by a total internal reflection. Moreover, we see that in the interval between the angles α_{p01} and α_{p12} the circuit R_{psub} coincides with the corresponding one to the envelope R_{pm} , and beyond its boundaries with R_{pM} . This feature of envelops allows optimization of the algorithm for determining the parameters of thin films in the envelope method [21-24]. In a symmetrical state of the structure in terms of reflection properties, the Brewster angles for the opposing surfaces of the same layer coincide and one of the corners (19) becomes imaginary

or hides by total internal reflection at the opposite boundaries of the layer. For s – wave the reflection circuit of clean substrate surface R_{ssub} , coincides with the envelope R_{sM} .

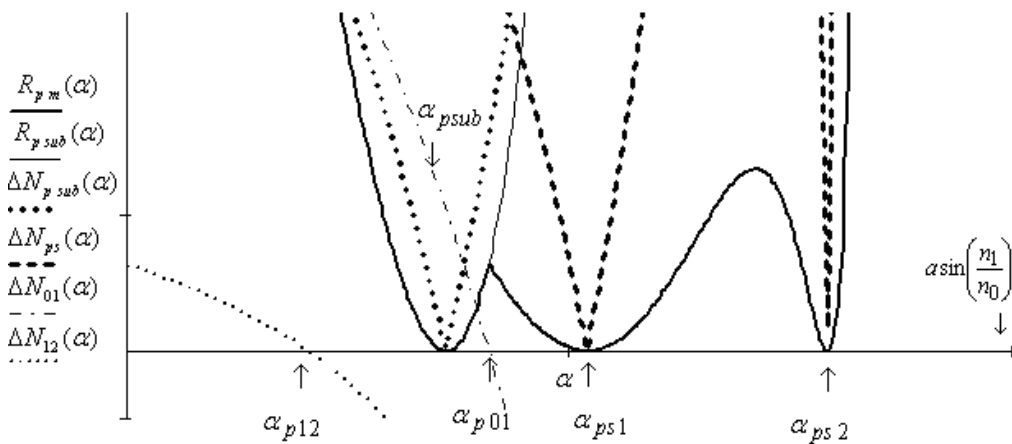


Fig. 2. Fragments of calculated angular circuits of envelopes $R_{pm,M}$, clean substrate surface R_{psub} and difference functions $\Delta N_{0,1,2}$, ΔN_{ps} , ΔN_{psub} for the p -wave by a single layer with the parameters $n_0 = 1.5$, $n_1 = 1.2$ and $n_2 = 1.15$

Figure 3a,b presents calculations of the dynamic shifts of angles α_{ps}, α_{ss} from the correlation between the refractive indices of the media. It can be seen in the range of $n_0 < n_2$ given that $n_1 \rightarrow n_0$ the angles $\alpha_{ps1} \rightarrow \frac{\pi}{2}$ and $\alpha_{ss} \rightarrow \frac{\pi}{2}$. The angles α_{ps}, α_{ss} may be hidden by total internal reflection at the angle $\arcsin\left(\frac{n_1}{n_0}\right)$ at the range $n_0 > n_2$ their maximum values are limited by $\arcsin\left(\frac{n_2}{n_0}\right)$.

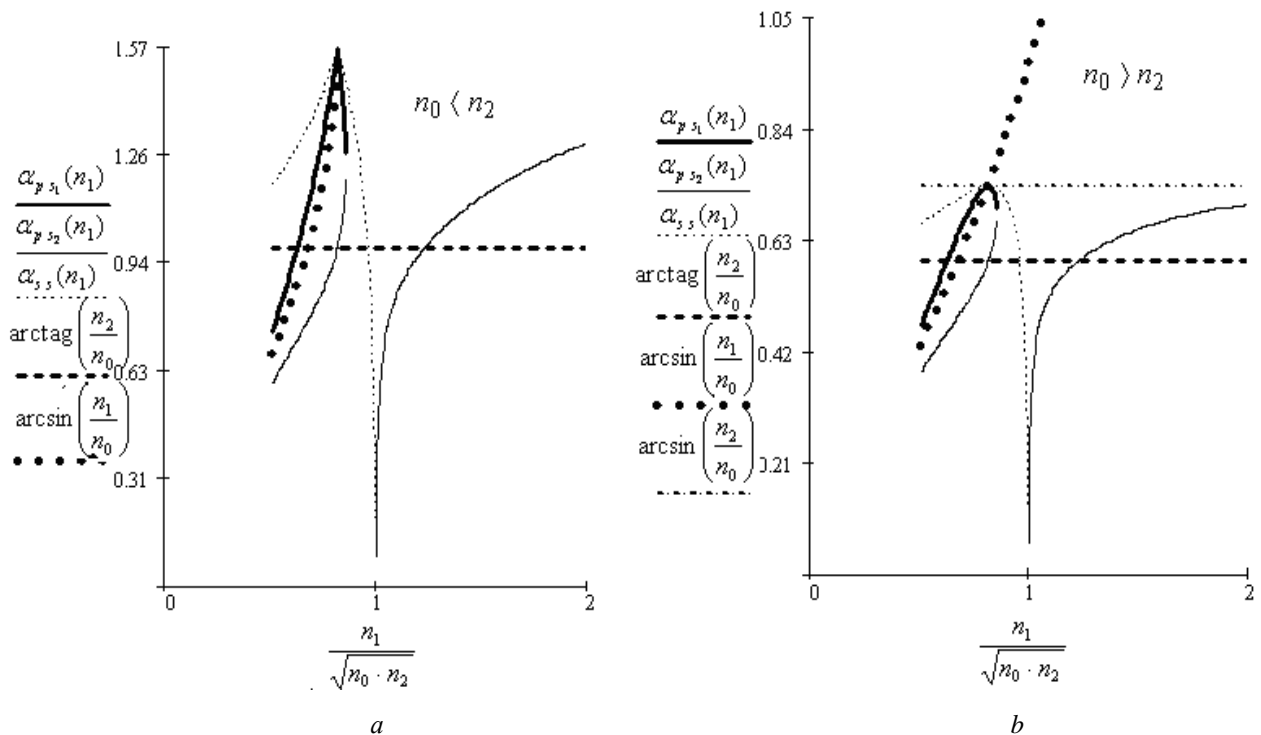


Fig. 3.a,b: The graphs of angles α_{ps}, α_{ss} , antireflection of the envelope circuit R_m for both wave polarizations depending on the ratio between the refractive index and the illustration of their manifestation limitations in the spectra by total internal reflection at the interface

They vanish in both polarizations if the refractive index of the film is $n_1 = \sqrt{n_0 n_2}$. If the refractive index of the structure $n_0 = 1$, the angles $\alpha_{ps1,2}$ may antireflect on both sides of the angle α_{psub} , depending on the relation between the value of the indices n_1 and n_2 . Full antireflection of a single-layer structure as a whole, when both equations (10) are performed simultaneously, depending on the relation between the refractive index, occurs provided that the phase thickness of the layer, multiple unpaired number of values $\delta = \pi$, when $n_0 > n_1 > n_2$ or $n_0 < n_1 < n_2$. The effect of absorption and layering will be discussed in a separate research work.

Conclusions

Suppression of impedance contrast of single boundaries at normal wave incidence are conditioned by the alignment of the optical characteristics of the contacting media, and at oblique incidence – by the Brewster character of reflection when the Fabry-Perot oscillations are decayed and the circuits of wave reflection by monolayer structure as a whole, clean substrate surface and the envelope extrema of multipath interference intersect at one point. In terms of antireflection of envelope minima of the Fabry-Perot interference, suppression of impedance contrast of binary boundaries is achieved by alignment of modules of wave reflection coefficients by opposite boundaries of the layer. Given the wave phase shifts on the opposite layer boundaries, full antireflection of the whole structure is achieved when the phase thickness, multiple of odd quantity $\delta = \pi$, given $n_0 > n_1 > n_2$ or $n_0 < n_1 < n_2$ and $\delta = 2\pi$ given $n_0 > n_1 < n_2$ or $n_0 < n_1 > n_2$. In the nonlinear dispersion area of layer it is possible to form a new type of antireflection window of interference envelope minima Fabry-Perot due to obstruction of resonant absorption of the reflectivity of the boundary between the plane-parallel coating and the substrate.

References

1. Born M, Wolf E. *Principles of Optics*. Moscow: Nauka 1973.
2. Macleod H.A. *Thin film optical filters*. Bristol: Hilger 1986.
3. Thelen Å. *Design of optical interference coatings*. New York: McGraw-Hill 1989.
4. Furman Sh. A, Tikhonravov A. V. *Basics of optics of multilayer systems*. Gif-sur-Yvette: Editions Frontiers 1992.
5. Bennet J. M. *Polarization*. In *Handbook of Optics*. Sponsored by the Optical Society of America. Michael Bass, editor in chief. – 2nd ed. McGraw: Hill. Inc. 1995; p. 5.1–5.28.
6. Willey R. *Practical Design and Production of Optical Thin Films*. Crc.Press 2002.
7. Kaiser N, Pulker H. K. *Optical Interference Coatings*. Berlin: Springer-Verlag 2003.
8. Al-Dilami Ahmed A., Vrublevsky I. A, Chernyakova K. V., Pykhir G. A. *Absorption of energy of electromagnetic radiation in interference in sulated structures with nanoporous alumina // Scient & Tecn PFMT 2014; 2(19): 96–9.*
9. Micheli D., Apollo C., Pastore R. and et al. *Electromagnetic characterization of composite materials and microwave absorbing modeling*. In: Reddy B editor. *Materials Science: Composite Materials. Advances in Nanocomposites – Synthesis, Characterization and Industrial Applications*. ISBN 978-953-307-165-7, Published: April 19, 2011 under CC BY-NC-SA 3.0 license.
10. Linkov L. M. et al. *New materials for screens of electromagnetic radiation*. *Doklady BGUIR 2004, 3: 152–167.*
11. Baskakov A. N. et al. *Resonance effects full interference absorption of wave energy in the subtle that weakly absorb layers // Letters to J of Technical Physics 1976, 2(19): 891–3.*
12. Kozar A. V. *Distribution of electric field intensity in multilayer systems of resonant type*. In: Kozar A. V., Kolesnikov W. S., Pirogov Y. A. Editors. *Bulletin of Moscow state University, Physics and astronomy 1978, 9(1): 78–86.*
13. Sokolovskyy I., Pokrovsky Yu. *Applied radiooptics. Theory and methods the resonant angular filtering*. – Kiev: Naukova Dumka, 1986.
14. Schopper H. *Zur Optik dünner doppelbrechender und dichroitischer Schichten // Zeitschrift für Physik 1952, 132(2): 146–70.*
15. Brewster D. *On the laws which regulate the polarisation of light by reflexion // Philos Trans 1815, 105: 125–30.*
16. Bass M editor. *Handbook of Optics (2)*. 2nd ed. New York: McGraw-Hill 1995.
17. Kosobutsky P. S. *Inversion of a nonmonotonic polarizational angular dependence of light reflection coefficient from a thin film on an absorbing substrate // J Appl Spectr 2005; 72(2): 277–9.*
18. Abeles F. *Methods for determining optical parameters of thin films*. In: Wolf E editor. *Progress in Optics (2)*. Amsterdam: North Holland 1963; p. 429–88.
19. Martinez-Anton J. *Simultaneous determination of film thickness and refractive index by interferential spectrogoniometry // Opt Commun 1966; 132(3–4): 321–8.*
20. Dyankov G. *Modified channeled spectrum for fast measurement of thin films // Appl Opt 2008; 47(4): 536–47.*
21. Kosobutskyy P. S. *Envelope method of Fabry-Perot spectra interferometry*. Lviv: Lvivska Polytechnika 2013.
22. Kosobutskyy P. S. *Physics bases for modeling the electromagnetic wave processes in optics / Kosobutskyy P. S., Karkulovska M. S., Sehedra M. S. – Lviv: Lvivska Polytechnika, 2003.*
23. Kosobutskyy P. S. *Extrema envelope function multibeam interference Fabry-Perot / Kosobutskyy P. S., Karkulovska M. S. – Part I. Properties and applied aspects for plane-parallel single-layer systems // Radioelectronics & Informatics J 2012, 4:90–4.*
24. Humphrey S. *Direct calculation of the optical constants for a thin film using a midpoint envelope // Appl Opt 2007; 46: 4660-6.*